ZIBELINE INTERNATIONAL™ PUBLISHING

Water Conservation and Management (WCM)

DOI: http://doi.org/10.26480/wcm.02.2021.71.77

ISSN: 2523-5664 (Print)
ISSN: 2523-5672 (Online)
CODEN: WCMABD

RESEARCH ARTICLE

CRUSHED CONCRETE AS ADSORPTIVE MATERIAL FOR REMOVAL OF PHOSPHATE IONS FROM AQUEOUS SOLUTIONS

Arega Genetie Abetu[a*] and Adisu Befekadu Kebede[b]

[a]Department of Hydraulic and Water Resource Engineering, School of Civil and Hydraulic, Institute of Technology, University of Gondar, Gondar P.O. Box 196, Ethiopia
[b]Department of Water Supply and Environmental Engineering, Faculty of Civil and Environmental Engineering, Jimma Institute of Technology, Jimma University, Jimma P.O. Box 378, Ethiopia
**Corresponding Author E-mail: genetiearega@yahoo.com*

ARTICLE DETAILS

Article History:

Received 23 July 2021
Accepted 24 August 2021
Available online 14 September 2021

ABSTRACT

The contamination of surface and groundwater with phosphate originating from industrial, agricultural and household wastewater remains a serious environmental issue in low-income countries. Currently, demolished concrete is mainly recycled as aggregate for reconstruction and conventional wastewater treatment systems for removing phosphate are expensive and complex. In this study, we were aiming at testing crushed concrete as an efficient adsorbent for the removal of phosphate from aqueous solutions, obtained from the demolition of construction site. It can reduce pollution and landfill disposal by converting construction waste into valuable products and an alternative solution for phosphate removal. Batch adsorption experiments were conducted using phosphate solutions to examine the adsorption kinetic as well as equilibrium conditions. Results show that the phosphate adsorption of all absorbents follows the adsorption isotherms with a varying phosphate concentration from 3 mg/L to 18 mg/L, and the adsorption isotherms data are fitted well by Langmuir equation as compared with the Freundlich isotherm. The maximum phosphate adsorption (97.67 %) was obtained at a contact time of 120 min, an initial phosphate concentration of 10 mg/L, and a solution pH of 4. The pseudo second-order equation describes the experimental data has good agreement, with a correlation value of R^2 = 0.99. The results obtained indicate that the environmentally available crushed concrete have a good adsorptive capacity for phosphate and shall be considered in future studies as test materials for phosphate removal from water in technical-scale experiment.

KEYWORDS

Adsorption, aqueous solution, crushed concrete, isotherm models, phosphate.

1. INTRODUCTION

Excessive phosphate discharge from manure, sludge sources, and chemical fertilizer applied to agricultural soils to runoff is the prominent source of water quality deterioration and nutrient enrichment. Heavily phosphate-laden waters impose hazardous risk to aquatic ecosystems (Tabbara, 2003). Municipal and industrial wastewaters are the main point sources for phosphate while run-off from agriculture is the dominant non-point source. Studies indicate that 4 to 15 mg/L phosphate may be contained in municipal wastewater, whereas effluent from chemical industries such as detergent manufacturing and metal coating processes may contain 14 to 25 mg/L phosphate (Arshadi et al., 2018).

According to the tolerable phosphate level in waters should not exceed 0.05 mg/L to maintain an ecologically sustainable status (Yadav et al., 2015). In such a case, to lower the phosphate loading in wastewater and runoff especially if local circumstances do not allow for advanced techniques such as membrane filtration became a challenge to local scientists and engineers.

The elimination of phosphate from water can be achieved via many processes, such as biological process, chemical precipitation, and adsorption methods (Tao et al., 2020; Lalley et al., 2016). In comparison, biological processes and chemical precipitation are expensive and result in a large amount of waste sludge to dispose of, involving high operating costs (Choi et al., 2014; Han et al., 2017). Therefore, it is of great interest to develop reliable technologies that utilize viable adsorbents to remove excess phosphate from water. It has been reported that due to its ease of application, economic feasibility, and high efficiency among the mentioned methods, adsorption is the most efficient process for the removal of phosphate from water (Acelas et al., 2014; Saki et al., 2019).

Studies on P-laden wastewater treatments have revealed adsorption to be a highly effective and easy method among the physicochemical treatment processes if materials are carefully chosen (Alemayehu et al., 2009; Mehrabi et al., 2016). Some of these adsorbents are nanoscale zerovalent iron (NZVI), rice husk and fruit juice, acid-activated red mud, granulated coal ash, aleppo pine, zirconium(IV) loaded fibrous, still slag produced, bone charcoal, Lanthanum hydroxide materials, aluminum sludge, modified multi-walled carbon nanotube with chitosan, manganese-laden

Quick Response Code	Access this article online	
	Website: www.www.watconman.org	**DOI:** 10.26480/wcm.02.2021.71.77

Cite the Article: Arega Genetie Abetu and Adisu Befekadu Kebede (2021). Crushed Concrete as Adsorptive Material for Removal of Phosphate Ions from Aqueous Solutions. *Water Conservation and Management, 5(2): 71-77.*

bio-char, marble waste, chitosan composited beads derived from crude oil refinery waste, iron-coated diatomite, halloysite nanotubes, and industrial solid waste bio-char (Tor and Cengeloglu, 2006; Asaoka and Yamamoto, 2010; Benyoucef and Amrani, 2011; Awual et al., 2011; Meyer et al., 2012; Ghaneian et al., 2014; Xie et al., 2014; Nawar et al., 2015; Huang et al., 2018; Jiang et al., 2018; Bouamra et al., 2018; Cui et al., 2019; Lyngsie et al., 2019; Qiu and Duan, 2019).

The properties of concrete that make it a good filter material is its high calcium content as calcium silicates and calcite and a porous surface structure. Reference describes the main mechanism of phosphate elimination as the release of calcium from tobermorite, a predominant calcium silicate hydrate in concrete, followed by the formation of hydroxyapatite (Berg et al., 2005). Hence, the type of concrete can determine its efficiency. Reference shows field-scale tests using 5 different types of crushed concretes (Sønderup et al., 2014). The highest sorption capacity is shown by gas concrete (19 mg P/g) and the lowest is shown by classic concrete (5.1 mg P/g).

However, no information is available on the adsorptive interactions between phosphate in the aqueous system and crushed concrete. Therefore, the objectives of this study were: (1) to examine the characteristics of the crushed concrete, (2) to investigate the phosphate sorption capacity of crushed concrete under a batch adsorption setup, (3) to determine kinetics of the adsorption reaction onto crushed concrete, and (4) to predict the adsorption process by using isotherm models.

2. Materials and Methods

2.1 Adsorbent Preparation and Characterization

Waste concrete was collected from a demolition construction site and the concrete waste was crushed using crushing machines (Concrete Crusher A35399). Next, the aggregates were sieved to obtain the desired sizes ranging between 5 mm to 30 mm (British Standard sieve BS410/1986) using a shaker (Endecotts Lombard Rd. London, model SW193BR, England). Crushed concrete samples in the range of sizes of 5 to 20 mm were accepted for use as adsorbents for the batch study. They are washed twice with distilled water to remove any contaminations, and then oven-dried at 105 ^{0}C for 24 h and stored in air-tight containers until the test.

Crushed concrete was scanned by an infinite focus microscope (Alicona). An infinite focus microscope can quantitatively measure surface texture or deviations in a surface character. Physico–chemical properties such as organic matter, moisture content, electrical conductivity and pH zero point of charges (pHzpc) were also measured according to (Penn et al., 2018).

2.2 Reagents Used and Adsorbate Preparation

All chemicals used in this experiments for preparing phosphate solutions and for analyzing adsorbed phosphate, such as KH_2PO_4, $C_6H_8O_6$, $(NH_4)_6Mo_7O_{24}{\cdot}4H2O$, $(SbO)K(C_4H_4O_6){\cdot}1/2H_2O$, H_2SO_4 were analytical reagent grade chemicals from Carl Roth (Karlsruhe, Germany). The varying concentrations of phosphate solution for adsorption experiments were prepared by diluting the stock solution (1000 mg L–1 phosphate).

A stock solution of potassium dihydrogen phosphate, KH_2PO_4 with a concentration of 1000 mg/L PO_4^{3-} and 99.9% purity, was diluted to a working solution with concentrations of 1 mg/L PO_4^{3-} to 100 mg/L PO_4^{3-} in 1000 mL of de-ionized water then labeled as 'phosphate solution or working solution' and stored in a tightly closed plastic bottle in a cool place (4 °C) until the experiments were commenced.

2.3 Batch Adsorption Studies

Measured concentration of the desired Phosphate ion prepared from the stock solution was place in 1000 ml of volumetric flask to make 100 ml of solution. The pH of the adsorbate solution was calibrated by buffer solution (pH =7 and 9) and adjusted to the desired value by adding 0.1M H_2SO_4 and NaOH solution and measured by a micro-processor pH meter model 210. The batch experiment was conducted by agitating of each adsorbent with 100 mL of phosphate solution of known concentration ranging from 1 mg L–1 to 100 mg L–1 in plastic acid-washed polypropylene bottles. The batch containers were shaken using a horizontal shaker at desired shaking speed to homogenize the samples and to accelerate the adsorption at a temperature of 22 ± 1 ^{0}C.

At the end of equilibrium time (24 h), the mixtures were filtered through 0.50 mm nylon mesh and the concentration of residual phosphate at equilibrium time was determined by the photometric method (Molybdenum blue method) and a spectrophotometer (Specord 40, Analytik Jena AG, Jena, Germany) at 850 nm (Murphy and Riley, 1962). Each experiment was conducted triplicate to check the repeatability of the experimental data, and data represent the mean value of the individual results. The amount of phosphate adsorbed at time t and the adsorbed amount qt were calculated from the mass balance equation:

$$qt = (co - ct) * \frac{V}{M} \quad (1)$$

Where, C_0 is the initial concentration of phosphate in contact with crushed concrete, C_t is the mass concentration of phosphate in the aqueous phase at time t and q_t is the amount of adsorbed phosphate per unit mass of crushed concrete (mg kg^{-1}), M is dry mass of the adsorbent (kg), and V the volume of solution (L).

2.4 Data analysis and Presentation

2.4.1 Adsorption Kinetics

In order to investigate the adsorption kinetics, pseudo-first order and pseudo-second-order and intra-particle diffusion models were applied for the estimation of rate constants (Ajmal et al., 2006).

Pseudo-first-order expression was employed as in Equation (2):

$$\log(q_e - q_t) = \log(q_e) - {}^{K_1 t}/_{2.0303}, \quad (2)$$

Where, K_1 is the first-order rate constant of adsorption (min−1); q_e (mg/g) and, q_t (mg/g) are the amount of phosphate adsorbed at equilibrium and at time t respectively. The values of K_1 and q_e can be obtained from the slope and the intercept of a linear straight-line plot of log (q_e − q_t) versus t.

The pseudo second-order equation can be written as shown in Equation (3): (Peleka and Deliyanni, 2009).

$$\frac{dq_t}{dt} = K_2(q_e - q_t)^2. \quad (3)$$

And integrating provided the linear pseudo-second order expression as Equation (4):

$$\frac{t}{q_t} = \frac{1}{x} + \frac{1}{q_e}t, \quad (4)$$

Where, qe (mg/g) and q_t (mg/g) are the amount of phosphate adsorbed at equilibrium and time t respectively; x = K_2qe^2 and K_2 is the rate constant of the pseudo second-order model (g/mgmin). The value of x and q_e can be obtained from the linear t/q_t vs. t plot.

The intra-particle diffusion equation can be expressed as shown in Equation (5).

$$q_t = K_{id}t^{0.5} + C \quad (5)$$

Where, q_t is the amount of phosphate adsorbed at time t, Kid (mg·g $^{-1}$ ·$min^{-1/2}$) is the intra-particle diffusion rate constant obtained from the slope of the plot q_t vs. $t^{0.5}$, and C (mg·g $^{-1}$) is the intercept of the plot, often referred to as the thickness of the boundary layer and obtained from the intercept of the plot (Chen et al., 2013).

2.4.2 Adsorption Isotherm

Various models can be employed to characterize the adsorption behavior of a given compound analyzing experimental data. Adsorption isotherms relate the adsorbed amount of phosphate to the equilibrium solution concentration at a constant temperature. These relations are also named 'quantity-intensity-relations'. Freundlich and Langmuir isotherms are the

most frequently used models to analyze experimental observations. These two non- linear isotherm models (Equations (6) and (7)) were applied to obtain the adsorption isotherm constants.

Langmuir equation: $$\frac{C_e}{q_e} = \frac{1}{q_m K_L} + \frac{C_e}{q_m} \quad (6)$$

Freundlich equation: $$\ln q_e = \ln K_F + \frac{1}{n}\ln C_e \quad (7)$$

Where, q_e (mg/g) is the specific amount of adsorbate (phosphate), and C_e (mg/L) is the adsorbate concentration in the liquid phase at equilibrium. The constants K_L (L/mg) and q_{max} (mg/g) of the Langmuir isotherm are indicative of adsorption energy and adsorption density respectively. K_F and n (dimensionless) are Freundlich constants and indicate the total adsorption capacity and intensity of adsorption respectively.

The Langmuir equation is also used to obtain RL, the separation factor, from the following expression: $R_L = \frac{1}{1 + K_L C_o}$ in which C_o (mg/L) is the initial concentration of phosphate in the solution. If $0 < R_L < 1$ then a favorable adsorption situation can be assumed, while $R_L > 1$ indicates an unfavorable adsorption, and $R_L = 1$ and $R_L = 0$ indicate a linear and irreversible adsorption isotherm respectively. The model equations were fitted to the experimental data using the Microsoft Excel solver function.

3. Results and Discussion

3.1 Adsorbents Characterization

Figure 1 shows crushed concrete has a crude surface, which indicates more adsorption sites. The specific surface area of crushed concrete was also identified as 35 m^2/m^3. The crushed concrete was examined by EDS (ED3000) and composed of 56 % oxygen, 18 % Si, 10 % Carbon, 10 % Ca, 2 % Al, 2 % K, and 1 % Mg.

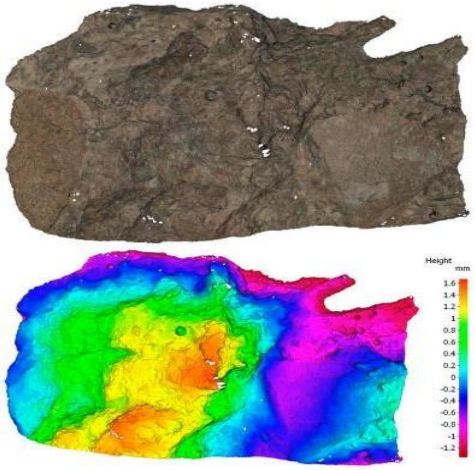

Figure 1: Crushed concrete scanning by infinite focused microscope

3.2 Effects of contact time

Designing an appropriate batch adsorption experiment is very important to get the rate at which the adsorption takes place, and the adsorption process' time dependence was described by varying the contact time between the adsorbates and the adsorbents' surface. Adsorption experiment was conducted to observe the effect contact time on removal efficiency crushed concrete. The removal efficiency of Phosphate at contact time interval of 20, 40, 60, 80, 100 and 120 minutes was carried out and found to be 95.31 %, 95.31 %, 97.28 %, 98.22 %, 98. 54 % and 99.42 % respectively. As it is well described in Figure 2, the percentage removal increased from 95.31 % to 99.42 % from 20 to 120 minutes of contact time.

The effect of contact time on phosphate removal by crushed concrete is presented in Figure 2. The phosphate capture on the surface of adsorbent was very rapid in the first 80 min, and equilibrium was attained after 120 min contact time. Increasing the contact time increased the uptake of phosphate, indicating the high affinity of phosphate to bare surfaces and a fast filling of active sites due to boundary layer diffusion. It can be observed from Figure 2 that the adsorption process had a rapid and a slow component. The rapid adsorption (up to 80 min) was based on the availability of active sites and a high phosphate concentration in the solution at the early stages of the experiment. The following slow adsorption is due to intra-particle diffusion and an according phosphate mass transfer onto crushed concrete. A similar finding has been reported in the literature (Du et al., 2017). The adsorption rate of the adsorbent usually increases rapidly during the initial reaction time and then slowly reaches equilibrium (Ghaedi et al., 2011). Previous researches reported that the phosphate capture on the surface of leftover coal was very rapid in the first 200 min, and equilibrium was attained after 720 min contact time (Mekonnen et al., 2020). This is attributed to a large amount of mesopores available for adsorption at the first contact time.

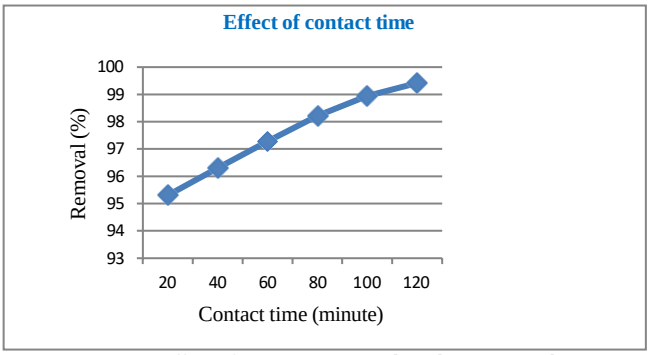

Figure 2: Effect of contact time on phosphate removal

3.3 Adsorption Kinetics

Commonly used three kinetic models, pseudo-first, pseudo-second-order models and inter-particle were employed to fit the experimental data. Optimized model parameter values are presented in Table 1. The equilibrium capacity as obtained from the fitting procedure employing the pseudo second-order model (qe) very well represented the measured value. The pseudo second-order model best represents the experimental data (R^2 = 0.99; Figure 3b), which can be taken as an indicator that chemisorption was the dominant process (Witek-krowiak et al., 2011; Pan et al., 2019). This would imply that the cause of phosphate adsorption onto the crushed concrete involves valency forces through sharing or exchanging electrons between sorbate and sorbent (Bhakat et al., 2006). Thus, the kinetics of phosphate adsorption on pumice was well described by the pseudo-second- order equation that indicates the rate-limiting step could be surface chemical adsorption involving valence forces through the sharing or exchange of electrons between adsorbent and adsorbate (Robati, 2013). Similar results were reported for phosphate removal from wastewater using palm fibers (*Phoenix dactylifera* L.) (Riahi et al., 2017).

Table 1: Calculated values of parameters for pseudo-first order, pseudo-second order, and the intra-particle diffusion kinetics model for phosphate adsorption onto crushed concrete

Kinetic Model	Parameters	Crushed Concrete
Pseudo-first-order	qe (mg/g)	0.123
	K_1 (min^{-1})	-0.0033
	R^2	0.96
Pseudo-second-order	qe (mg/g)	0.485
	K_2 ($g.mg^{-1}$,min^{-1}	178.59
	R^2	0.99
Intra-particle diffusion	K_{id} ($mg.mg^{-1}.min^{-1/2}$	0.0135
	C	9.5875
	R^2	0.93

Intra-particle diffusion is also responsive to the diffusion mechanism of the adsorbate in the solution. If the plots for the intra-particle diffusion qt vs. $t^{0.5}$ of Equation (5) for crushed concrete is leaner and pass through the origin, then the intra-particle diffusion model is the sole rate-limiting step; otherwise, an adsorptive process other than intra-particle diffusion can occur (Ahn et al., 2009). In our case, the linear plot of qt vs. $t^{0.5}$ (Figure 5) did not pass through the origin but was linear in some points. Therefore, this validates that intra-particle diffusion was not the only rate-limiting step, and non-diffusive reaction also occurred between the phosphate ion and crushed concrete.

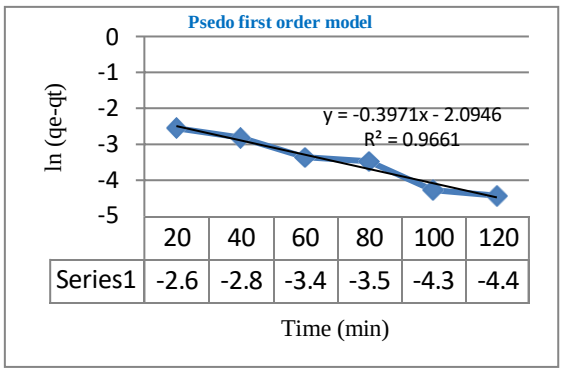

(a)

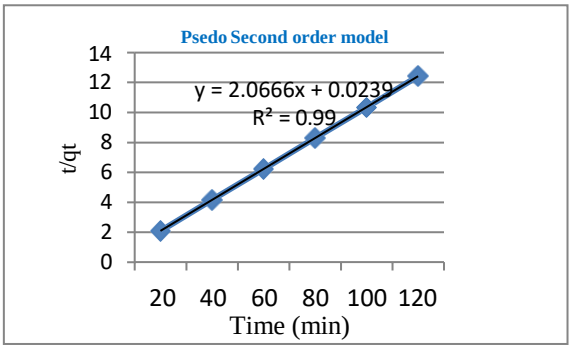

(b)

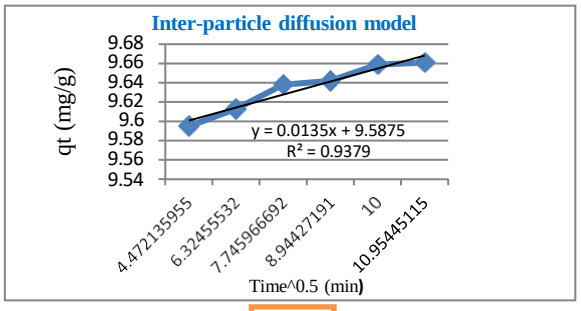

(c)

Figure 3: Kinetic of phosphate adsorption process: (a) Pseudo first order, (b) Pseudo second order and (c) Inter-particle diffusion

3.3 Effect of Adsorbent Dose

The effect of adsorbent dose on the phosphate removal onto crushed concrete was investigated in the range of 75 – 275 mg and the result was presented in Figure 4. The percent of phosphate removal increased (from 91.6 % to 99.7 %) with the increase of the dose of crushed concrete (from 75 to 275 mg). On the other side, the mass uptake per unit adsorbent (q, mg/g) was decreasing (from 18.33 mg/g to 3.99 mg/g) with increasing the dose of crushed concrete from 75 to 275 mg, which can be related to the higher abundance of sorption sites.

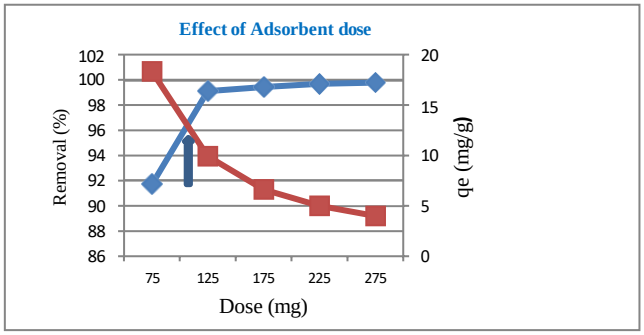

Figure 4: Effect of adsorbent dose on the removal efficiency of phosphate

It is also evident from Figure 4 that maximum optimum removal of 99.7 % was taking place at adsorbent dose of 0.275 g for which the sharp break in the curve of sorbent doses was reaching the optimal dose at 0.275 g, showing the trade-off between removal percentage and capacity of crushed concrete dose. Sorbent dose in excess of this value has a limited effect on the removal of additional phosphate ion from adsorption system or little to increase adsorptive capacity of sorbent material under the study. The *KD* values for phosphate adsorption onto pumice, which determined at pH 7, increased with an increase in adsorbent dose, indicating the heterogeneity of the surface of pumice (Rahdar et al., 2019). Increasing the dose of sorbent increased the total removal of P by increasing the availability of sorption sites. Similar trends have been also reported by other authors (Burianek et al., 2014; Molle et al., 2003).

3.4 Effect of Initial Concentration

The variation in phosphate removal by crushed concrete as a function of the initial phosphate concentration is presented in Figure 5 in the supplementary material. It was noticed that the percent removal of phosphate decreased (from 98.97 % to 96.7 %) with an increase in initial phosphate concentration (from 3 to 18 mg·L −1). This is because the resistance to the up-taking of the adsorbate onto the adsorbents' surfaces is higher, and the active site for adsorption gets saturated at higher concentrations. In contrast, phosphate removal capacity, qe, increased with increasing the initial phosphate concentration due to the higher driving forces provided by the higher initial concentrations, which were able to resist the mass transfer between the solid surface and aqueous solution, which enables the adsorbate to remain on the surface of the adsorbents (Lin et al., 2018).

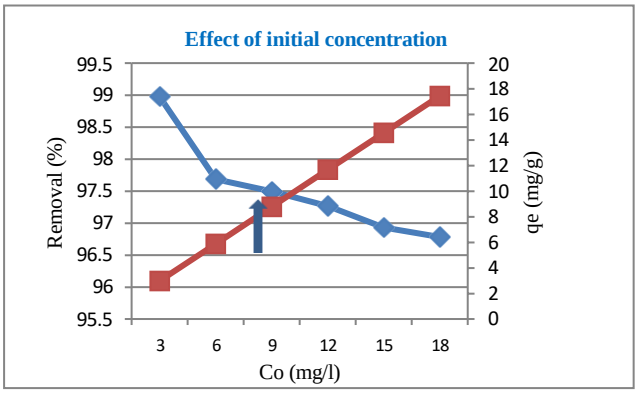

Figure 5: Effect of initial concentration on the removal efficiency of phosphate

As tried to describe in Figure 5 above, the maximum removal efficiency of 98.97 % was obtained at lower initial phosphate ion concentration of 3 mg/l and the maximum adsorption density was observed at higher phosphate concentration of 18 mg/l., found an exponential tendency: increasing initial concentration correlates with a higher sorption of Phosphate, as this interaction is stronger with increasing initial concentration. This is in line with previous equilibrium adsorption capacity experiments, which suggest that higher solute concentrations could encourage other mechanisms such as greater boundary concentrations which in turn lead to double layer adsorption and complex formation (Cucarella and Renman, 2009).

3.5 Effect of pH

The effect of pH on phosphate adsorption onto crushed concrete for this study is presented in Figure 6 in supplementary data. The percentage of phosphate removed from the aqueous solution decreased (from 98.68 % to 98.5 %) as the pH of the solution increased from 4 to 9 indicating that the adsorption of phosphate is likely to be based on physical interactions between the surfaces of the adsorbents and adsorbate. Previous studies indicate that the amount of Ca^{2+}ions leaching from the adsorbent decreases with an increase in pH value of the initial solution (Gan et al., 2009; Yin et al., 2011). At the lower pH range adsorption increases at sites with a variable charge (e.g., – COOH, $-NH_3$) because of increasing protonation. At high pH values, the competition with OH ions increases, and phosphate adsorption decreases. Similar reports confirm that phosphate removal is less efficient under alkaline conditions (Bui et al., 2018; Huang et al., 2014).

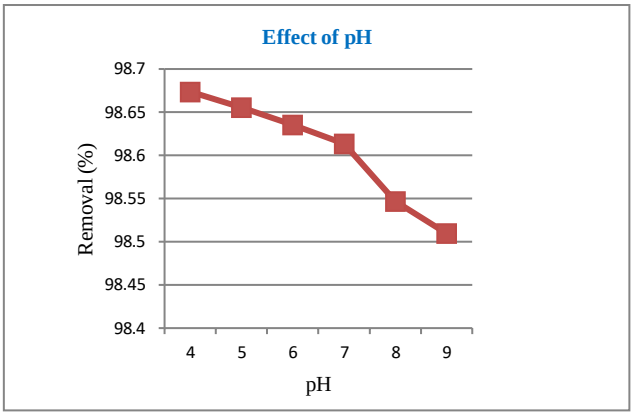

Figure 6: Effect of pH on the removal efficiency of phosphate

3.6 Effect of stirring speed

The effect of the stirring speed of the sorbent/sorbate system in phosphate adsorption was studied at 50,100, 150, 200, 250 and 300 rpm for 120 minutes of contact time, 0.100 g of crushed concrete in 100 ml of the solution containing 10 mg/l of phosphate at pH 3 at temperature 25^{0}C. As it is well described below, in the Figure 7, the percent adsorption increased from 95.09 %, 95.95 %, 96.34 %, 97.13 %, 97.88 % and 98.1 % with respective increase of shaking speed from 50 to 300 rpm. A maximum of 98.1 % removal was achieved at 300 rpm.

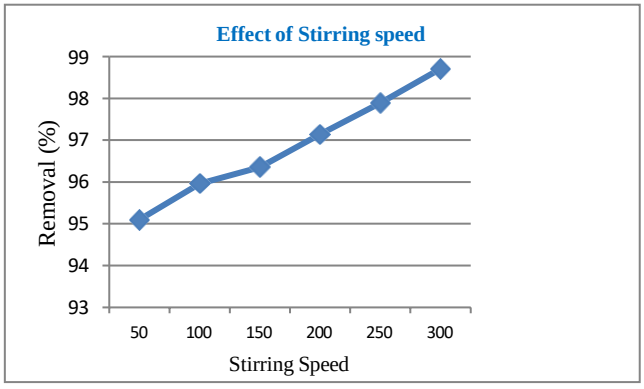

Figure 7: Effect of stirring speed on the removal efficiency of phosphate

Phosphate adsorption onto pumice increased with increasing agitation speed, reaching a maximum of 94.6% ± 1.1% removal at 200 r/min (Yohannis et al., Taffere, 2020). The increase in the percentage of phosphate removal is due to the dispersal of the adsorbent particles in the aqueous solution, which leads to reduced boundary mass transfer resistance that increases the percent removal of phosphate (Baraka et al., 2012).

3.7 Adsorption Isotherm

Analysis of the relationship between the adsorption capacity of the materials (Crushed Concrete) and different phosphate concentrations at equilibrium was performed using the equations of Langmuir (Equation (6)) and Freundlich (Equation (7)). The Freundlich model assumes that adsorption occurs on a heterogeneous surface through multilayer adsorption, and the adsorbed amount increases with increasing equilibrium concentrations. In opposite, the Langmuir model assumes an asymptotic approach to monolayer surface coverage. The isotherm plots of the equilibrium adsorption of phosphate are graphically presented in Figure 8, and the parameters values derived from the isotherm models and the parameters of determination are demonstrated in Table 2. It was found that among the tested materials, adsorption onto the granular form of crushed concrete was more pronounced than onto powder form. From the obtained optimization procedure it became evident that the Langmuir isotherm equation (R^2 = 0.978) described the system better than the Freundlich isotherm equation (R^2 = 0.935).

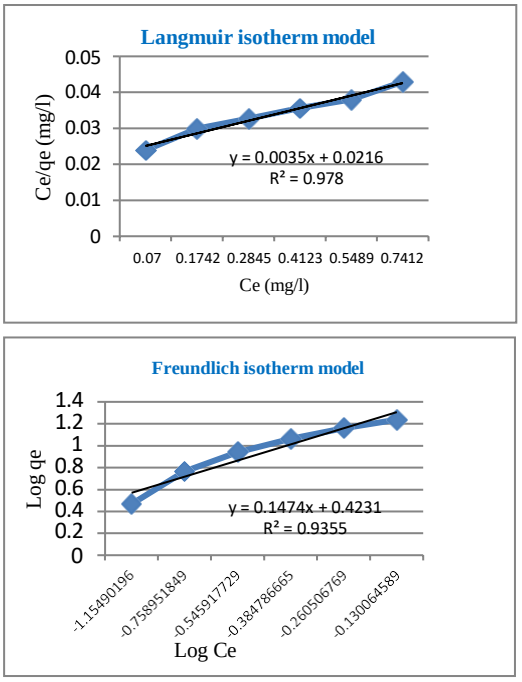

Figure 8: Adsorptive isotherm of phosphate on crushed concrete

Table 2: Adsorption isotherm parameters for the adsorption of phosphate onto crushed concrete

Isotherm	Freundlich				Langmuir			
Parameters	K_F ((mg·g^{-1}) (mg·L^{-1})) 1/n)$^{-1}$	1/n	nF	R^2	KL (l/mg^{-1})	RL	R^2	qmax (mg/g)
Value	2.65	0.147	6.8	0.935	1.35	0.039-0.198	0.978	28.5

The n-value of the Freundlich isotherm lies between 1 and 10, which is a good indicator for favourable adsorption (Pengthamkeerati et al., 2008). From the results obtained in Table 2, RL values for the Langmuir and 1/n values for the Freundlich isotherms were less than unity, and this elucidates that the adsorption of phosphate onto crushed concrete is favourable. Furthermore, the value of 1/n, which was obtained from the slope of the linear plot of logqe vs. logCe of the Freundlich isotherm, was below unity implying that chemisorption is the governing process (Foo and Hameed, 2010). The separation factor, RL as obtained from the Langmuir isotherm model was lower than unity, which likewise indicating to a favourable adsorption process (Zhou et al., 2019).

4. Conclusions

The study was used, cost-effective, demolished of construction material, and easily accessible crushed concrete to recover phosphate from aqueous solution. Design parameters such as initial phosphate concentration, initial solution pH, adsorbent dose, and contact time were optimized to obtain the highest possible removal. Adsorption of phosphate was highly pH dependent and the study results showed that the removal efficiency increased with deceasing the adsorbate and pH; and increasing the adsorbent dose, contact time and Stirring speed. The adsorption kinetics for phosphate removal could be well described by the pseudo-second-order equation with a correlation value of R^2 = 0.99 which revealed that, chemisorption was the dominant process. The Langmuir and Dubinin Radushkevich isotherms better described the adsorption process than Freundlich the isotherm model. The Langmuir RL value satisfied the condition 0< RL<1 and confirmed the favorability of adsorption process. Similarly, Freundlich isotherms adsorption constant value 1/n obtained to be 0.147 in the range of 0 and 1and reflected favorable adsorption. Besides, the isotherm adsorption constant, n = 6.8 (greater than 1 unity) and is an indicative chemisorptions.

References

Acelas, N.Y., Martin, B.D., López, D., Jefferson, B. 2014. Selective Removal of Phosphate from Wastewater Using Hydrated Metal Oxides Dispersed within Anionic Exchange Media. Chemosphere, 119, 1353–1360

Ahn, C.K., Park, D., Woo, S.H., Park, J.M. 2009. Removal of Cationic Heavy Metal from Aqueous Solution by Activated Carbon Impregnated with Anionic Surfactants. J. Hazard. Mater., 164, 1130–1136. [CrossRef]

Ajmal, M., Ali, R., Rao, K., Ahmad, R., Khan, M.A. 2006. Adsorption Studies on Parthenium Hysterophorous Weed: Removal and Recovery of Cd (II) from Wastewater. J. Hazard. Mater., B135, 242–248, doi:10.1016/j.jhazmat.2005.11.054.

Alemayehu, E., Lennartz, B. 2009. Virgin Volcanic Rocks: Kinetics and Equilibrium Studies for the Adsorption of Cadmium from Water. J. Hazard. Mater., 169, 395–401, doi:10.1016/j.jhazmat.2009.03.109.

Arshadi, M., Eskandarloo, H., Azizi, M., Abbaspourrad, A., Abdolmaleki, M.K., Eskandarloo, H., Azizi, M., Abbaspourrad, A. 2018. Synthesis of Highly Monodispersed, Stable, and Spherical NZVI of 20−30 Nm on Filter Paper for the Removal of Phosphate from Wastewater: Batch and Column Study. ACS Sustain. Chem. Eng., 6, 11662–11676, doi:10.1021/acssuschemeng.8b01885.

Asaoka, S., Yamamoto, T. 2010. Characteristics of Phosphate Adsorption onto Granulated Coal Ash in Seawater. Mar. Pollut. Bull., 60, 1188–1192, doi:10.1016/j.marpolbul.2010.03.032.

Awual, R., Jyo, A., Ihara, T., Seko, N. 2011. Enhanced Trace Phosphate Removal from Water by Zirconium (IV) Loaded Fibrous Adsorbent. Water Res., 45, 4592–4600, doi:10.1016/j.watres.2011.06.009.

Baraka, A.M., El-Tayieb, M.M., El Shafai, M., Mohamed, N.Y. 2012. Sorptive removal of phosphate from wastewater using activated red mud. Aust J Basic Appl Sci., 6: 500-510.

Benyoucef, S., Amrani, M. 2011. Adsorption of Phosphate Ions onto Low Cost Aleppo Pine Adsorbent. Desalination, 275, 231–236, doi:10.1016/j.desal.2011.03.004.

Berg, U., Donnert, D., Ehbrecht, A., Bumiller, W., Kusche, I., Weidler, P. and Nüesch, R. 2005. "Active filtration" for the elimination and recovery of phosphorus from waste water, Colloids and Surfaces A: Physicochemical and Engineering Aspects, 265(1-3), 141-148.

Bhakat, P. B., Gupta, A. K., Ayoob, S., and Kundu, S. 2006. Investigations on arsenic(V) removal by modified calcined bauxite, Colloids and Surfaces A: Physicochemical and Engineering Aspects, 281(1–3), 237–245.

Bouamra, F., Drouiche, N., Abdi, N., Grib, H., Mameri, N., Lounici, H. 2018. Removal of Phosphate from Wastewater by Adsorption on Marble Waste: Effect of Process Parameters and Kinetic Modeling. Int. J. Environ. Res., 12, 13–27, doi:10.1007/s41742-018-0065-3

Bui, T.H., Hong, S.P., Yoon, J. 2018. Development of Nanoscale Zirconium Molybdate Embedded Anion Exchange Resin for Selective Removal of Phosphate. Water Res., 134, 22–31, doi:10.1016/j.watres.2018.01.061.47.

Burianek, P., Skalicky, M., Grunwald, A. 2014. Phosphates adsorption from water by recycled concrete. GeoSci. Eng., LX, 1–8.

Chen, J., Cai, Y., Clark, M., Yu, Y. 2013. Equilibrium and Kinetic Studies of Phosphate Removal from Solution onto a Hydrothermally Modified Oyster Shell Material. PLoS ONE, 8, e60243

Choi, J., Ryu, J., Kwon, K., Song, M., Lee, S., Kim, S., Lee, S. 2014. Adsorption of Ammonium Nitrogen and Phosphate onto Basanite and Evaluation of Toxicity. Water Air Soil Pollut., 125.

Cucarella, V., Renman, G. 2009. Phosphorus sorption capacity of filter materials used for on-site wastewater treatment determined in batch experiments–a comparative study. J. Environ. Qual., 3, 381–392.

Cui, X., Li, H., Yao, Z., Shen, Y., He, Z., Yang, X., Ng, H.Y., Wang, C.H. 2019. Removal of Nitrate and Phosphate by Chitosan Composited Beads Derived from Crude Oil Refinery Waste: Sorption and Cost-Benefit Analysis. J. Clean. Prod., 207, 846–856, doi:10.1016/j.jclepro.2018.10.027

Du, X., Han, Q., Li, J., Li, H. 2017. The Behavior of Phosphate Adsorption and Its Reactions on the Surfaces of Fe–Mn Oxide Adsorbent. J. Taiwan Inst. Chem. Eng., 76, 167–175, doi:10.1016/j.jtice.2017.04.023.

Foo, K.Y., Hameed, B.H. 2010. Insights into the Modeling of Adsorption Isotherm Systems. Chem. Eng. J., 156, 2–10, doi:10.1016/j.cej.2009.09.013.

Gan, F., Zhou, J., Wang, H., Du, C., Chen, X. 2009. Removal of phosphate from aqueous solution by thermally treated natural palygorskite. Water Res. 43, 2907e2915. https://doi.org/10.1016/j.watres.2009.03.051.

Ghaedi, M., Hassanzadeh, A., Kokhdan, S.N. 2011. Multiwalled carbon nanotubes as adsorbents for the kinetic and equilibrium study of the removal of Alizarin red S and morin. J. Chem. Eng. Data 56, 2511e2520. https://doi.org/10.1021/ je2000414.

Ghaneian, M.T., Ghanizadeh, G., Alizadeh, M.T.H., Ehrampoush, M.H., Said, F.M. 2014. Equilibrium and Kinetics of Phosphorous Adsorption onto Bone Charcoal from Aqueous Solution. Environ. Technol., 35, 882–890, doi:10.1080/09593330.2013.854838.

Han, C., Lalley, J., Iyanna, N., Nadagouda, M.N. 2017. Removal of Phosphate Using Calcium and Magnesium-Modified Iron-Based Adsorbents. Mater. Chem. Phys., 198, 115–124.

Huang, W.Y., Li, D., Liu, Z.Q., Tao, Q., Zhu, Y., Yang, J., Zhang, Y.M. 2014. Kinetics, Isotherm, Thermodynamic, and Adsorption Mechanism Studies of La(OH)3-Modified Exfoliated Vermiculites as Highly Efficient Phosphate Adsorbents. Chem. Eng. J., 236, 191–201, doi:10.1016/j.cej.2013.09.077.

Huang, Y., Lee, X., Grattieri, M., Macazo, F.C., Cai, R., Minteer, S.D. 2018. A Sustainable Adsorbent for Phosphate Removal: Modifying Multi-Walled Carbon Nanotubes with Chitosan. J. Mater. Sci., 53, 12641–12649, doi:10.1007/s10853-018-2494-y.

Jiang, D., Chu, B., Amano, Y., Machida, M. 2018. Removal and Recovery of Phosphate from Water by Mg-Laden Biochar: Batch and Column Studies. Colloids Surf. A Physicochem. Eng. Asp., 558, 429–437, doi:10.1016/j.colsurfa.2018.09.016.

Lalley, J., Han, C., Li, X., Dionysiou, D.D., Nadagouda, M.N. 2016. Phosphate Adsorption Using Modified Iron Oxide-Based Sorbents in Lake Water: Kinetics, Equilibrium, and Column Tests. Chem. Eng. J., 284, 1386–1396.

Lin, J., Jiang, B., Zhan, Y. 2018. Effect of Pre-Treatment of Bentonite with Sodium and Calcium Ions on Phosphate Adsorption onto Zirconium-Modi Fi Ed Bentonite. J. Environ. Manag., 217, 183–195. [CrossRef]

Lyngsie, G., Katika, K., Fabricius, I.L., Hansen, H.C.B., Borggaard, O.K. 2019. Phosphate Removal by Iron OxideCoated Diatomite: Laboratory Test of a New Method for Cleaning Drainage Water. Chemosphere, 222, 884–890, doi:10.1016/j.chemosphere.2019.01.158.

Mehrabi, N., Soleimani, M., Sharififard, H., Yeganeh, M.M. 2016. Optimization of Phosphate Removal from Drinking Water with Activated Carbon Using Response Surface Methodology (RSM). Desalination Water Treat., 57, 15613–15618, doi:10.1080/19443994.2015.1070763.

Mekonnen, D.T., Alemayehu, E., Lennartz, B. 2020. Removal of Phosphate Ions from Aqueous Solutions by Adsorption onto Leftover Coal, Water, 12, 1381; doi:10.3390/w12051381.

Meyer, D., Chazarenc, F., Andre, Y., Barca, C., Ge, C., Nantes, M. De, Kastler, A., Universite, L.U. 2012. Phosphate Removal from Synthetic and Real Wastewater Using Steel Slags Produced in Europe. Water Res., 26, 2376–2384, doi:10.1016/j.watres.2012.02.012.

Molle, P., Lienard, A., Grasmick, A., Lwema, A. 2003. Phosphorus retention in subsurface constructed wetlands: Investigations focused on calcareous materials and their chemical reactions. Water Sci. Technol., 48, 75–83.

Murphy, J., Riley, J.P. 1962. A modified single solution method for the determination of phosphate in nature waters. Anal. Chem. ACTA 1962, 27, 31–36.

Nawar, N., Ahmad, M.E., El Said, W.M., Moalla, S.M.N. 2015. Adsorptive

Removal of Phosphorous from Wastewater Using Drinking Water Treatment-Alum Sludge (DWT-AS) as Low Cost Adsorbent. Am. J. Chem. Appl., 2, 79–85.

Pan, J., Gao, B., Song, W., Xu, X., Yue, Q. 2019. Modified Biogas Residues as an Eco-Friendly and EasilyRecoverable Biosorbent for Nitrate and Phosphate Removals from Surface Water. J. Hazard. Mater., 382, doi:10.1016/j.jhazmat.2019.121073.

Peleka, E.N., Deliyanni, E.A. 2009. Adsorptive Removal of Phosphates from Aqueous Solutions. Desalination, 245, 357–371, doi:10.1016/j.desal.2008.04.050.

Pengthamkeerati, P., Satapanajaru, T., Chularuengoaksorn, P. 2008. Chemical Modification of Coal Fly Ash for the Removal of Phosphate from Aqueous Solution. Fuel, 87, 2469–2476, doi:10.1016/j.fuel.2008.03.013.

Penn, C.J., Bowen, J.M. 2018. Design and Construction of Phosphorus Removal Structures for Improving Water Quality; Springer: Cham, Switzerland, ISBN 978-3-319-58658-8

Qiu, B., Duan, F. 2019. Synthesis of Industrial Solid Wastes/Biochar Composites and Their Use for Adsorption of Phosphate: From Surface Properties to Sorption Mechanism. Colloids Surf. A Physicochem. Eng. Asp., 571, 86–93, doi:10.1016/j.colsurfa.2019.03.041

Rahdar, S., Taghavi, M., Khaksefidi, R., Ahmadi, S. 2019. Adsorption of arsenic (V) from aqueous solution using modified saxaul ash: isotherm and thermodynamic study. Appl Water Sci., 9: 87. doi:10.1007/s13201-019-0974-0.

Riahi, K., Chaabane, S., Thayer, B.B. 2017. A kinetic modeling study of phosphate adsorption onto Phoenix dactylifera L. date palm fibers in batch mode. J Saudi Chem Soc., 21: S143-S152. doi:10.1016/j.jscs.2013.11.007.

Robati, D. 2013. Pseudo-second-order kinetic equations for modeling adsorption systems for removal of lead ions using multi-walled carbon nanotube. J Nanostruct Chem., 3: 55.

Saki, H., Alemayehu, E., Schomburg, J., Lennartz, B. 2019. Halloysite Nanotubes as Adsorptive Material for Phosphate Removal from Aqueous Solution. Water, 11, 1–10, doi:10.3390/w11020203.

Sønderup, M., Egemose, S., Hoffmann, C., Reitzel, K. and Flindt, M. 2014. Modeling phosphorus removal in wet ponds with filter zones containing sand or crushed concrete, Ecological Engineering, 66, 52-62.

Tabbara, H. 2003. Phosphorus loss to runoff water twenty-four hours after application of liquid swine manure or fertilizer. J. Environ. Qual., 32, 1044–1052.

Tao, X., Huang, T., Lv, B. 2020. Synthesis of Fe/Mg—Biochar Nanocomposites for Phosphate Removal. Materials, 13, 816. [CrossRef]

Tor, A., Cengeloglu, Y. 2006. Removal of Congo Red from Aqueous Solution by Adsorption onto Acid Activated Red Mud. J. Hazard. Mater., 138, 409–415, doi:10.1016/j.jhazmat.2006.04.063.

Witek-krowiak, A., Szafran, R.G., Modelski, S. 2011. Biosorption of Heavy Metals from Aqueous Solutions onto Peanut Shell as a Low-Cost Biosorbent. Desalination, 265, 126–134, doi:10.1016/j.desal.2010.07.042.

Xie, J., Wang, Z., Lu, S., Wu, D., Zhang, Z., Kong, H. 2014. Removal and Recovery of Phosphate from Water by Lanthanum Hydroxide Materials. Chem. Eng. J., 254, 163–170, doi:10.1016/j.cej.2014.05.113.

Yadav, D., Kapur, M., Kumar, P., Mondal, M.K. 2015. Adsorptive Removal of Phosphate from Aqueous Solution Using Rice Husk and Fruit Juice Residue. Process Saf. Environ. Prot., 94, 402–409. [CrossRef]

Yin, H., Yun, Y., Zhang, Y., Fan, C. 2011. Phosphate removal from wastewaters by a naturally occurring, calcium-rich sepiolite. J. Hazard Mater. 198, 362e369. https://doi.org/10.1016/j.jhazmat.2011.10.072.

Yohannis, F. and Taffere, A. 2020. Adsorptive Removal of Phosphate From Wastewater Using Ethiopian Rift Pumice: Batch Experiment. Ethiopian Environment and Forest Research Institute, Jimma Research Center, Jimma, Ethiopia. Air, Soil and Water Research, 13: 1–12.

Zhou, H., Bhattarai, R., Li, Y., Li, S., Fan, Y. 2019. Utilization of Coal Fly and Bottom Ash Pellet for Phosphorus Adsorption: Sustainable Management and Evaluation. Resour. Conserv. Recycl., 149, 372–380, doi:10.1016/j.resconrec.2019.06.017.